Effect of different kinds of SiC fibers on microwave absorption and mechanical properties of SiC_f/SiC composites

Zhaowen Ren (rzw0911@mail.nwpu.edu.cn)
Northwestern Polytechnical University School of Science

Wancheng Zhou
State Key Laboratory of Solidification Processing, Northwestern Polytechnical University, Xi'an 710072, Shaaxi, China

Yuchang Qing
State Key Laboratory of Solidification Processing, Northwestern Polytechnical University, Xi'an 710072, Shaanxi, China

Shichang Duan
Shaanxi Huaqin Technology Industry Co., Ltd.

Qinlong Wen
Northwestern Polytechnical University

Yingying Zhou
School of Materials Engineering, Xi'an Aeronautical University, Xi'an 710077

Yanyu Li
State Key Laboratory of Solidification Processing, Northwestern Polytechnical University, Xi'an 710072Northwestern Polytechnical University

Research Article

Keywords: SiCf/SiC composites, microwave absorption, mechanical property, SiC fibers

Posted Date: May 15th, 2020

DOI: https://doi.org/10.21203/rs.3.rs-27933/v1

Version of Record: A version of this preprint was published at Journal of Materials Science: Materials in Electronics on August 6th, 2020. See the published version at https://doi.org/10.1007/s10854-020-

04129-5.

Abstract

The SiC fibers are essential for designing microwave absorption and mechanical properties of multifunctional composites. In this study, SLF, KD-II and KD-S SiC fibers were used to fabricate SiC f /SiC composites. The SLF SiC fibers are composed by amorphous SiOC. The KD-II and KD-S SiC fibers exhibit higher crystallizations and free carbon content. The conductivity of SLF, KD-II and KD-S SiC fibers are 0.0127, 1.184 and 0.1316 S/cm, respectively. The flexural strength of SLF, KD-II and KD-S SiC f /SiC composites are 147.77, 322.57 and 248.16 MPa, respectively. The microwave absorption property of the SLF SiC f /SiC composites can be obtained over -25 dB with a thickness of 2.3 mm and the effective absorption bandwidth (EAB) below -10 dB reaches 3.72 GHz with the thickness of 2.7 mm. In contrast, the KD-II SiC f /SiC composites only reach -3.6 dB in the whole X band when the thickness varies from 2 to 2.9 mm. KD-S SiC f /SiC composites can be obtained over -9dB with the thickness of 2mm and the EAB below -7 dB reaches 4.12 GHz with a thickness of 2.2 mm. The mechanisms of mechanical, microwave absorption and penitential applications for SiC f /SiC composites are also discussed.

1. Introduction

Nowadays, as the development of microwave technology, electromagnetic pollution usually appears in daily life. Numerous researches have been devoted to designing and implementing excellent electromagnetic absorption materials[1–5]. In recently years, ceramics composites with excellent microwave absorption properties have increasingly attracted attentions, such as SiC nanowires reinforced SiOC ceramic, Si_3N_4-SiCN ceramics composites[6] and Fe_3O_4 nanoparticles on MXenes[7]. Continuous fiber reinforced ceramics matrix composites (CFRCMCs) were believed to be the most prospective multifunctional composites due to their high mechanical strength, stability under high temperature, low densities and oxidation resistance properties[8–10]. Therefore, SiC fiber reinforced SiC ceramic matrix composites can be promising candidates of multifunctional materials with microwave absorption and mechanical properties.

The microwave absorption and mechanical properties of SiC CFRCMCs depend on complex permittivity, electrical conductivity and free carbon content of SiC fibers, as well as interphase and matrix. The SiC ceramics matrix can be fabricated by chemical vapor infiltration (CVI)[11], precursor impregnation and pyrolysis (PIP)[12], liquid silicon infiltration (LSI)[13] and melt infiltration (MI)[14]. Among these techniques, the PIP method has many advantages, for instance, the designable molecular precursor of polymer derived ceramics (PDC), safe in operation and the feasibility of manufacture in large complex components. Thus, the PIP method should be a better way to fabricate the multifunctional SiC_f/SiC composites.

Different types of SiC fiber significantly affect the properties of SiC_f/SiC composites. Up to now, the SiC fibers have developed three generations[15–17]. The first generation of SiC fibers is Nicalon 200 from Nippon Carbon and Tyranno LOX-M from UBE industries, etc. The second generation of SiC fibers is Hi-

Nicalon from Nippon Carbon, Tyranno ZE from UBE Industries, and so on. The third generation of SiC fibers is Tyranno SA 1 from UBE Industries, Sylramic from COI ceramics, and so forth. The oxygen contents in fibers came down as the generation developed. The first generation oxygen content could go as high as 12 wt% with the maximum limit temperature only 1200 °C. The excessive oxygen content of SiC fibers was harmful. Since the active-oxidation could cause coarsening of β-SiC crystals at high temperature[18]. The oxygen content of the second generation is lower than 2 wt% with enhanced limit temperature of about 1300 °C. However, the second generation also has poor oxidation-resistance property due to the high C/Si ratio of 1.5. The oxygen content of the third generation is lower than 1 wt% with the maximum temperature over 1700 °C and the C/Si ratio only about 1. Moreover, the third generation has high crystallinity and density. The polycrystalline SiC fibers can give rise to better elastic modulus and tensile strength of fibers[19]. All of the above mentioned SiC fibers are from Japan, America and Germany. However, with the efforts of Chinese researchers, SiC fibers can be fabricated in China at present.

In this research, the SLF, KD-II and KD-S SiC fibers are all produced in China and represent first, second and third generation of SiC fibers, respectively. These SiC fibers were used as reinforcements. The polycarbosilane (PCS) was used as precursor of SiC ceramics matrix. In order to avoid the influence of interphase on properties of SiC_f/SiC composites, the interphase on the surface of fibers was not fabricated in the present work. We systematically investigated the properties of SiC fibers and the effects of different SiC fibers on microwave absorption and mechanical properties of SiC_f/SiC composites.

2. Experimental

2.1 Raw materials of SiC_f/SiC composites

The SLF fibers and PCS powders were bought from Suzhou CeraFil Ceramic Fiber Co., Ltd. KD-II and KD-S fibers were purchased from the National University of Defense and Technology (NUDT). The general properties of three three types of SiC fibers are listed in Table 1[9, 20]. The SiC fibers were used as reinforcement and fabricated into 2.5D with a volume fraction of 35%. Additionally, the PCS/xylene solution was prepared at 50 wt%.

Table 1
properties of KD-S, KD-II and SLF SiC fibers

SiC fibers	C/Si atomic ratio	Bulk density (g/cm^3)	Diameter (μm)	Tensile strength (GPa)	Tensile modulus (GPa)
KD-S	1.05	2.85	11	2.6	320
KD-II	1.4	2.75	12	2.9	280
SLF	/	2.47	12	2.2	185

2.2 Preparation of SiC_f/SiC composites with different SiC fibers

Firstly, these three kinds of 2.5D SiC fibers were ultrasonic cleared in acetone solution for 15 min. Afterwards, the 2.5D SiC fibers were dipped into PCS/xylene solution for 30 min in the vacuum infiltration oven and then dried at 80 °C for 3 h in the vacuum drying oven. After dried, the samples were pyrolyzed in a vacuum sintering furnace at 1000 °C for 2 h. SiC_f/SiC composites were fabricated by the PIP procedure and repeated until the weight gain less than 1% per cycle.

2.3 Characterization of SiC_f/SiC composites

The density and open porosity of these SiC_f/SiC composites were measured by Archimedes' principle. Phase compositions of SiC fibers were analyzed by X-ray diffraction (X'Pert PRO MPD, PANalytical. Almelo, the Netherlands, Cu-Kα radiation). The crystalline grain size *L* of SiC fibers was calculated by Scherrer's Equation[21]:

$$L = \frac{K\lambda}{B\cos\theta} \qquad (1)$$

where *B* is the full width at half maximum (FWHM) of the (1 1 1) peak. *θ* is the Bragg's diffraction angle. *K* is the Scherrer's constant. λ is the X-ray wavelength.

Additionally, the crystallinity of SiC fibers was calculated by the following equation with XRD spectra:

$$X_c = \frac{I_c}{I_a + I_c} \times 100\% \qquad (2)$$

where I_c represents the crystal diffraction peak area. I_a represents amorphous diffraction peak area. The judging standard of crystal diffraction peak is FWHM less than 3.0.

The flexural strength of the SiC_f/SiC composites was characterized by the three-point-bending method using a universal testing machine (Haida Qualitative Analysis, HD-609B) at room temperature. Mechanical samples were cut into 40mm × 4mm × 3 mm. This universal testing machine had a cross head speed of 0.5 mm/min with a span of 30 mm. The surface of SiC fibers and fracture surfaces of SiC_f/SiC composites were observed by scanning electron microscope (Model VEGA3 SBH, TESCAN, Brno, Czech) with energy dispersion spectroscopy (EDS). The conductivity of SiC fibers can be calculated by the equation:

$$\sigma = \frac{L}{RS} \qquad (3)$$

where L and S is the length and cross section area of a bunch of SiC fibers, respectively. One bunch of fibers consisted of 1000 SiC fibers. R is the resistance of one bunch of SiC fibers, which was measured by a resistant tester.

The complex permittivity of SiC_f/SiC composites was measured at the frequency between 8.2 and 12.4 GHz using the waveguide method with a vector network analyzer (Agilent Technologies E8362B). The dimension of complex permittivity samples was 22.86mm × 10.16mm × 2.0 mm.

3. Results And Discussion

3.1 Microstructure of SiC fibers

The surface and cross-section morphologies of different SiC fibers are shown in Fig. 1. The surface of the SiC fibers is smooth and homogeneous. The diameters of SiC fibers are all about 12 μm. The SiC fibers were cut to observe cross-section, which was shown a dense morphology. Many particles with a small size can be seen on the cross-section of fibers.

Compositional elements of surface and cross-section of different SiC fibers at selected regions in Fig. 1 were measured by EDS, seen in Fig. 2. By comparing SLF, KD-II and KD-S SiC fibers, Fig. 2 (a) and (b) show that the content of oxygen element in SLF fibers is 17.21% on the surface and 10.36% in cross-section. Therefore, SLF SiC fibers satisfy the characteristic of high oxygen content in the first generational and process a large amount of SiOC phase[22]. In contrast, the oxygen content of KD-S SiC fibers is only 2.34% on surface and 3.03% in cross-section. The content of Si element increased with the content of oxygen element decreasing in the SLF, KD-II and KD-S SiC fibers. Additionally, from SLF, KD-II to KD-S, the ratio of C/Si is reduced. However, the content of C element in KD-II SiC fibers is the highest in the cross-section.

The different properties of these three types of SiC fibers can be reflected by polycrystalline microstructure[19]. As shown in Fig. 3, the XRD revealed the crystalline structure of different SiC fibers. The crystallinity and crystallite size of β-SiC crystallite for SLF, KD-II and KD-S SiC fibers are shown in Table 2. The XRD patterns demonstrate that the microstructures of SiC fibers are mainly formed by β-SiC at peaks of 35.74°, 41.50°, 60.14°, 71.97° and 75.71°, which are indexed to (1 1 1), (2 0 0), (2 2 0), (3 1 1) and (2 2 2) lattices, respectively. It can be seen that the SLF SiC fibers present three main diffraction peaks at 35.74°, 60.14° and 71.97°, which were assigned to the (1 1 1), (2 2 0) and (3 1 1) planes of the amorphous β-SiC phase, respectively. The sharp XRD peaks observed for the KD-II and KD-S SiC fibers clearly confirm the larger crystallite size (4.4 nm and 4.1 nm) of β-SiC than that of the SLF SiC fibers (1.4 nm). Moreover, other peaks were indexed as the (2 0 0) and (2 2 2) planes of the β-SiC appeared in

KD-II and KD-S SiC fibers. As same as the first generation of SiC fibers, the SLF fibers are almost amorphous, according to the broad minor peaks[23]. In contrast, the KD-II and KD-S SiC fibers have high crystallinity with 83.92% and 87.76%, respectively.

Thanks to the amorphous phase and high oxygen content, the free carbon conductive network in the SLF fibers will be separated by Si-C-O phase[16]. Therefore, as shown in Table 3, the conductivity of SLF fibers is only 0.0127 S/cm. The conductivity of KD-II fibers is 1.1811 S/cm owing to the larger C/Si atomic ratio[19] and the conductive network of carbon-rich layers. The conductivity of KD-S fibers is 0.1316 S/cm due to the lower C and O content.

Table 2
Crystallinity and crystallite size of β-SiC for SLF, KD-II and KD-S SiC fibers

Properties	SLF	KD-II	KD-S
Crystallinity (%)	≈ 0	83.92	87.76
Crystallite size (nm)	1.4	4.4	4.1

Table 3
Conductivity of SLF, KD-II and KD-S SiC fibers

	SLF	KD-II	KD-S
Conductivity(S/cm)	0.0127	1.1811	0.1316

3.2 Mechanical properties and microstructure of SiC_f/SiC composites

Mechanical properties of SiC_f/SiC composites with SLF, KD-II and KD-S SiC fibers are listed in Table 4. The flexure strength of the KD-S and KD-II SiC_f/SiC composites are 248.16 MPa and 322.57 MPa, respectively. The KD-II SiC_f/SiC composites exhibited the best mechanical properties comparing to the SLF and KD-S SiC_f/SiC composites, owing to the fact that massive free carbon networks generated by the high content of C in the KD-II SiC fibers. Under the same fabricating condition, the density and open porosity of SLF, KD-II and KD-S SiC_f/SiC composites are pretty similar. However, the flexure strength of SLF SiC_f/SiC composites is only 147.77 MPa. It indicates that the growth of crystallites and high crystallinity are beneficial to enhance the flexure strength of SiC_f/SiC composites.

Table 4
Properties of SiC_f/SiC composites SLF, KD-II and KD-S SiC fibers

SiC_f/SiC composites	Density (g/cm^3)	Open porosity (%)	Flexural strength (MPa)	Displacement (mm)
SLF	1.99	12.2	147.77	0.240
KD-II	2.13	12.5	322.57	0.333
KD-S	1.98	13.04	248.16	0.275

The stress-displacement curves obtained from the bending test for SiC_f/SiC composites with different kinds of SiC fibers are shown in Fig. 4. The load on the SLF, KD-II and KD-S SiC_f/SiC composites decreases sharply as reaching the peak value. It is revealed that all kinds of SiC fibers reinforced SiC_f/SiC composites appear a typical brittle fracture behavior. It can be concluded that the bonding strength between three types of SiC fibers and the matrix was strong.

The fracture morphologies of SiC_f/SiC composites with SLF, KD-II and KD-S fibers were shown in Fig. 5. As illustrated in Fig. 5 (a), the fracture surface of SLF SiC_f/SiC composites was plane and there are no fibers pull-out phenomenon appearance due to the strong bonding at the surface between matrix and SLF SiC fibers. The fracture surface of KD-II SiC_f/SiC composites exhibits step-shaped appearances, shown in Fig. 5 (b). In Fig. 5 (c), the step-shaped fracture and fibers pull-out can be discovered in the fracture surface of KD-S. According to the fracture morphologies, the matrix densification of SLF, KD-II and KD-S SiC_f/SiC composites are similar. With the same content of matrix and SiC fibers in SiC_f/SiC composites, the different mechanical properties should be caused by different kinds of SiC fibers.

3.3 Dielectric properties of SiC_f/SiC composites with different SiC fibers

The complex permittivity ($\varepsilon = \varepsilon' - j\varepsilon''$) of SiC_f/SiC composites with various SiC fibers was measured at the frequency range of X band (8.2–12.4 GHz). The real part of permittivity (ε') is correlated with polarization and the imaginary part of permittivity (ε'') in reference to the ability of dielectric loss and electrical conductivity[24]. The loss tangent (tanδ) of SiC_f/SiC composites were calculated by $\tan\delta = \varepsilon'/\varepsilon''$[25], which represents the microwave absorption ability of SiC_f/SiC composites[26].

As shown in Fig. 4, both the real and imaginary permittivity of KD-II SiC_f/SiC composites reveal a decreasing trend as the frequency increases in the whole X band. It can be indicated that the KD-II SiC_f/SiC composites possess frequency dispersion effect and a broad microwave absorption band. The complex permittivity of SLF and KD-S SiC_f/SiC composites almost keeps constant in the measured range, in which the values are 7.9-4.0j and 11.6-9.2j at the frequency of 10 GHz respectively. Compared with SLF and KD-S SiC_f/SiC composites, the KD-II SiC_f/SiC composites possess much higher imaginary permittivity

and loss tangent. The real and imaginary part of permittivity of KD-II SiC_f/SiC composites is 12.6 and 25.0 at 10 GHz, respectively, and the loss tangent of it is in the range of 1.7–2.2 in the whole X band. It suggests that the KD-II SiC_f/SiC composites has the strongest microwave absorption ability.

The SiC_f/SiC composites are composited by SiC fibers, interface and SiC matrix. Therefore, the real and imaginary permittivity of SiC_f/SiC composites can be illustrated as Lichtencker's logarithmic equations [8, 24]:

$$\ln \varepsilon' = v_f \ln \varepsilon'_f + v_m \ln \varepsilon'_m + v_i \ln \varepsilon'_i \quad (4)$$

$$\ln \varepsilon'' = v_f \ln \varepsilon''_f + v_m \ln \varepsilon''_m + v_i \ln \varepsilon''_i \quad (5)$$

where v_f, v_m and v_i are volume contents, ε'_f, ε'_m and ε'_i are real permittivities, and ε''_f, ε''_m and ε''_i imaginary permittivities of SiC fiber, SiC matrix and interface, respectively. In this experiment, the interface was not fabricated and the porosity and density of SiC matrix was similar as shown in Table 4. Additionally, the SLF, KD-II and KD-S SiC fibers were all fabricated into 2.5D with volume fraction of 35% and the process of manufacture SiC_f/SiC composites was under the same experimental condition. Consequently, the real and imaginary part of SiC_f/SiC composites are mainly dependent on SiC fibers.

On the one hand, there are lots of interfaces around SiC nano-crystals, free carbons and amorphous SiOC phase. Additionally, the dipoles from defect in SiC nano-crystals and free carbons in SiC fibers[24]. The KD-II and KD-S SiC fibers with high crystallinity have more grain boundaries and free carbons. Therefore, the higher real permittivity of KD-II and KD-S SiC_f/SiC composites owing to the polarization from interfaces among the grain boundary and dipoles in the KD-II and KD-S SiC fibers under the X band. On the other hand, according to the Debye theory[27], the imaginary part of permittivity can be decided by the conductivity, which can be calculated by the following equation:

$$\varepsilon'' = \frac{\sigma}{2\pi\varepsilon_0 f} \quad (6)$$

where σ is the electrical conductivity, ε_0 is the dielectric constant in vacuum and f is the frequency of the electromagnetic wave. According to the above analysis, the imaginary part of permittivity of SiC_f/SiC composites in this experiment is proportional to the conductivity of SiC fibers. As shown in Table 3, the conductivity of KD-II SiC fibers 1.1811 S/cm is the highest. Therefore, the higher electrical conductivity of KD-II SiC fibers gives rise to the larger imaginary part of KD-II SiC_f/SiC composites.

3.4 Microwave absorption properties of SiC_f/SiC composites

The microwave absorption property of SLF, KD-II and KD-S SiC_f/SiC composites are evaluated by the reflection loss (RL) values, which is based on the transmission line theory. The RL values can be calculated as the following equations:

$$RL(\mathrm{dB}) = 20 \log \left| \frac{Z_{in} - Z_0}{Z_{in} + Z_0} \right| \quad (7)$$

$$Z_0 = \sqrt{\frac{\mu_0}{\varepsilon_0}} \quad (8)$$

$$Z_{\mathrm{in}} = Z_0 \sqrt{\frac{\mu_r}{\varepsilon_r}} \tanh\left[j\left(\frac{2\pi f t}{c}\right) \sqrt{\mu_r \varepsilon_r} \right] \quad (9)$$

where Z_0 is the characteristic impedance of free space, Z_{in} is the input impedances of the interface between SiC_f/SiC composites and free space. μ_0 and ε_0 are the permeability and permittivity of vacuum. μ_r and ε_r are the measured relative permeability and permittivity. Because of negligible magnetic properties of SiC, the value of μ_r in this experiment, is taken as 1. Consequently, the RL values of dielectric microwave absorption SiC_f/SiC composites can be calculated by complex permittivity and thickness in X band.

Generally, the high loss tangent can give rise to the better microwave absorption abilities. However, the optimum impedance matching between the free space and the surface of microwave absorption material leads microwave reflection reduced, and then enhanced the energy loss of the incident microwave. For optimum matching impedance, it demands that the input impedance Z_{in} equal with free space impedance Z_0 as far as possible. The input impedance Z_{in} of SLF, KD-II and KD-S SiC_f/SiC composites with a thickness of 2.9 mm are shown in Fig. 5.

The Z_{in} value of the KD-II SiC_f/SiC composites is in the range of 63.15–75.12 Ω. The higher difference between Z_{in} and Z_0 leads to the stronger reflection of incident microwave on the surface of the SiC_f/SiC composites. Therefore, the KD-II SiC_f/SiC composites possess poor microwave absorbing properties, as shown in Fig. 6 (c) and (d). In X band, the KD-II SiC_f/SiC composites has only − 3.6 dB RL values from 2 to 2.9 mm thickness and there is no reflection loss peak appearance. On the contrary, the Z_{in} value of SLF SiC_f/SiC composites is the highest, in the range of 328.65–178.70 Ω, and processes the lowest deviation between Z_{in} and Z_0. As a consequence, most of the microwave incidence into SLF SiC_f/SiC composites. As shown in Fig. 6 (a) and (b), the RL values of SLF SiC_f/SiC composites can be obtained over − 25 dB with a thickness of 2.3 mm and the effective absorption bandwidth (EAB) below − 10 dB reaches 3.72 GHz (from 8.68 to 12.40 GHz) with a thickness of 2.7 mm. The Z_{in} value of the KD-S SiC_f/SiC composites is in the range of 141.80-85.39 Ω. That deviation between Z_{in} and Z_0 is higher than that of KD-II SiC_f/SiC composites and lower than that of SLF SiC_f/SiC composites. As shown in Fig. 6 (c) and (f), the RL values of KD-S SiC_f/SiC composites can be obtained over − 9dB with a thickness of 2 mm and the

EAB below − 7 dB reaches 4.12 GHz (from 8.28 GHz to 12.40 GHz), indicating more than 84% microwave absorption[26], with the thickness of 2.2 mm.

With the same SiC matrix, the SLF SiC_f/SiC composites possess the optimum microwave absorption property due to the amorphous Si-O-C structure and low conductivity of SLF fibers. Additionally, the interfacial polarization is generated by the massive amount of amorphous SiOC and free carbon in SLF fibers. When microwave propagates into the SLF SiC_f/SiC composites, a large number of dipoles generated from free carbon, amorphous SiOC and amorphous SiC. The dipoles could cause displacement polarization or steering polarization with the changed electromagnetic wave. The dipoles polarization gradually lagged behind the changes. At this time, the energy of electromagnetic wave can be consumption[4, 28]. Instead, a large amount of interface generated between free carbon in the KD-II and KD-S fibers lead displacement polarization or steering of dipoles easy and consume less electromagnetic wave energy under the alternating microwave.

4. Conclusion

In summary, the SiC_f/SiC composites fabricated with SLF, KD-II and KD-S SiC fibers by PIP method have similar density and open porosity values. The SLF SiC fiber possessed a large amount of oxygen and amorphous phase. The KD-II and KD-S SiC fiber exhibit higher crystallizations and higher free carbon contents than SLF SiC fibers. KD-II SiC_f/SiC composites have the highest flexural strength with a value of 322.57 MPa and possess the worst microwave absorption property owing to the massive carbon in the fibers. SLF SiC_f/SiC composites possess the best microwave absorption property due to the best impedance matching with air and the lowest flexural strength can be ascribed to the poor strength of SLF SiC fibers.

The microwave absorption property of the SLF SiC_f/SiC composites can be obtained over − 25 dB with a thickness of 2.3 mm and the effective absorption bandwidth (EAB) below − 10 dB reaches 3.72 GHz with a thickness of 2.7 mm, indicating its potential application in the structural and absorbing field.

Above all, the SLF SiC fiber can be used as reinforcement for microwave absorption structure composites. But the interphase on the surface of SLF SiC fibers was necessary to the flexural strength enhancement. Because of the high loss tangent and mechanical property, KD-II SiC fibers are better used as the absorption layer in the multi-layered radar absorbing structures composites field. The KD-S SiC fibers possess medium levels of microwave absorption and mechanical properties. Therefore, further studies should focus on the matrix and interphase modification of KD-S composites.

Declarations

Acknowledgments

This work was financially supported by National Nature Science Foundation of China (Grant No. 51701148), Natural Science Basic Research Plan in Shaanxi Province of China (Grant No. 2019JQ-916)

References

[1] Qing Y, Min D, Zhou Y, et al. Graphene nanosheet- and flake carbonyl iron particle-filled epoxy–silicone composites as thin–thickness and wide-bandwidth microwave absorber[J]. Carbon. 2015, 86: 98-107.

[2] Qing Y, Wen Q, Luo F, et al. Graphene nanosheets/BaTiO3 ceramics as highly efficient electromagnetic interference shielding materials in the X-band[J]. Journal of Materials Chemistry C Materials for Optical & Electronic Devices. 2016, 4: 371-375.

[3] Nan H, Qing Y, Gao H, et al. Synchronously oriented Fe microfiber & flake carbonyl iron/epoxy composites with improved microwave absorption and lightweight feature[J]. Composites Science and Technology. 2019, 184: 107882.

[4] Qing Y, Zhou W, Luo F, et al. Titanium carbide (MXene) nanosheets as promising microwave absorbers[J]. Ceramics International. 2016, 42(14): 16412-16416.

[5] Qing Y, Wen Q, Luo F, et al. Temperature dependence of the electromagnetic properties of graphene nanosheet reinforced alumina ceramics in the X-band[J]. Carbon An International Journal Sponsored by the American Carbon Society. 2016, 4: 4853-4862.

[6] Li Q, Yin X, Feng L. Dielectric properties of Si3N4–SiCN composite ceramics in X-band[J]. Ceramics International. 2012, 38(7): 6015-6020.

[7] Liu P, Yao Z, Ng V M H, et al. Facile synthesis of ultrasmall Fe3O4 nanoparticles on MXenes for high microwave absorption performance[J]. Composites Part A: Applied Science and Manufacturing. 2018, 115: 371-382.

[8] Mu Y, Zhou W, Wang H, et al. Mechanical and dielectric properties of 2.5D $SiC_f/SiC–Al_2O_3$ composites prepared via precursor infiltration and pyrolysis[J]. Materials Science and Engineering: A. 2014, 596: 64-70.

[9] Duan S, Zhu D, Jia H, et al. Enhanced mechanical and dielectric properties of SiCf/SiC composites with silicon oxycarbide interphase[J]. Ceramics International. 2018, 44(1): 631-637.

[10] Gao H, Luo F, Nan H, et al. Improved mechanical and microwave absorption properties of SiC fiber/mullite matrix composite using hybrid SiC/Ti3SiC2 fillers[J]. Journal of Alloys and Compounds. 2019, 791: 51-59.

[11] Mu Y, Zhou W, Wang C, et al. Mechanical and electromagnetic shielding properties of SiCf/SiC composites fabricated by combined CVI and PIP process[J]. Ceramics International. 2014, 40(7): 10037-

10041.

[12] Mu Y, Zhou W, Hu Y, et al. Improvement of mechanical and dielectric properties of PIP-SiCf/SiC composites by using Ti3SiC2 as inert filler[J]. Ceramics International. 2015, 41(3): 4199-4206.

[13] Wan F, Pizada T J, Liu R, et al. Structure and flexural properties of 3D needled carbon fiber reinforced carbon and silicon carbide (C/C-SiC) composites fabricated by gaseous and liquid silicon infiltration[J]. Ceramics International. 2019, 45(14): 17978-17986.

[14] Guo W, Ye Y, Bai S, et al. Preparation and formation mechanism of C/C–SiC composites using polymer-Si slurry reactive melt infiltration[J]. Ceramics International. 2020, 46(5): 5586-5593.

[15] Pengren W, Fengqi L, Hao W, et al. A Review of Third Generation SiC Fibers and SiCf/SiC Composites[J]. Journal of Materials Science & Technology. 2019.

[16] Bunsell A R, Piant A. A review of the development of three generations of small diameter silicon carbide fibres[J]. Journal of Materials Science. 2006, 41(3): 823-839.

[17] Honglei Wang S G S P. KD-S SiC_f/SiC composites with BN interface fabricated by polymer infiltration and pyrolysis process[J]. Journal of Advanced Ceramics. 2018, 7(02): 169-177.

[18] Shimoo T, Okamura K, Morisada Y. Active-to-passive oxidation transition for polycarbosilane-derived silicon carbide fibers heated in Ar-O2 gas mixtures[J]. Journal of Materials Science. 2002, 37(9): 1793-1800.

[19] Gou Y, Jian K, Wang H, et al. Fabrication of nearly stoichiometric polycrystalline SiC fibers with excellent high-temperature stability up to 1900°C[J]. Journal of the American Ceramic Society. 2018, 101(5): 2050-2059.

[20] Wang H, Zhou X, Peng S, et al. Fabrication, microstructures and properties of SiCf/SiC composites prepared with two kinds of SiC fibers as reinforcements[J]. New Carbon Materials. 2019, 34(2): 181-187.

[21] Lim D J, Marks N A, Rowles M R. Universal Scherrer equation for graphene fragments[J]. Carbon. 2020, 162: 475-480.

[22] Wen Q, Yu Z, Riedel R. The fate and role of in situ formed carbon in polymer-derived ceramics[J]. Progress in Materials Science. 2019: 100623.

[23] Dong S M, Chollon G, Labrugère C, et al. Characterization of nearly stoichiometric SiC ceramic fibres[J]. Journal of Materials Science. 2001, 36(10

): 2371-2381.

[24] Li Q, Yin X, Zhang L, et al. Effects of SiC fibers on microwave absorption and electromagnetic interference shielding properties of SiCf/SiCN composites[J]. Ceramics International. 2016, 42(16):

19237-19244.

[25] Gao H, Luo F, Wen Q, et al. Effect of preparation conditions on mechanical, dielectric and microwave absorption properties of SiC fiber/mullite matrix composite[J]. Ceramics International. 2019.

[26] Duan S, Zhu D, Dong J, et al. Enhanced mechanical and microwave absorption properties of SiCf/SiC composite using aluminum powder as active filler[J]. Journal of Alloys and Compounds. 2019, 790: 58-69.

[27] Chen D, Luo F, Gao L, et al. Dielectric and microwave absorption properties of divalent-doped $Na_3Zr_2Si_2PO_{12}$ ceramics[J]. Journal of the European Ceramic Society. 2018, 38(13): 4440-4445.

[28] Guo X, Feng Y, Lin X. The dielectric and microwave absorption properties of polymer-derived SiCN ceramics[J]. Journal of the European Ceramic Society. 2018, 38(4): 1327-1333.

Figures

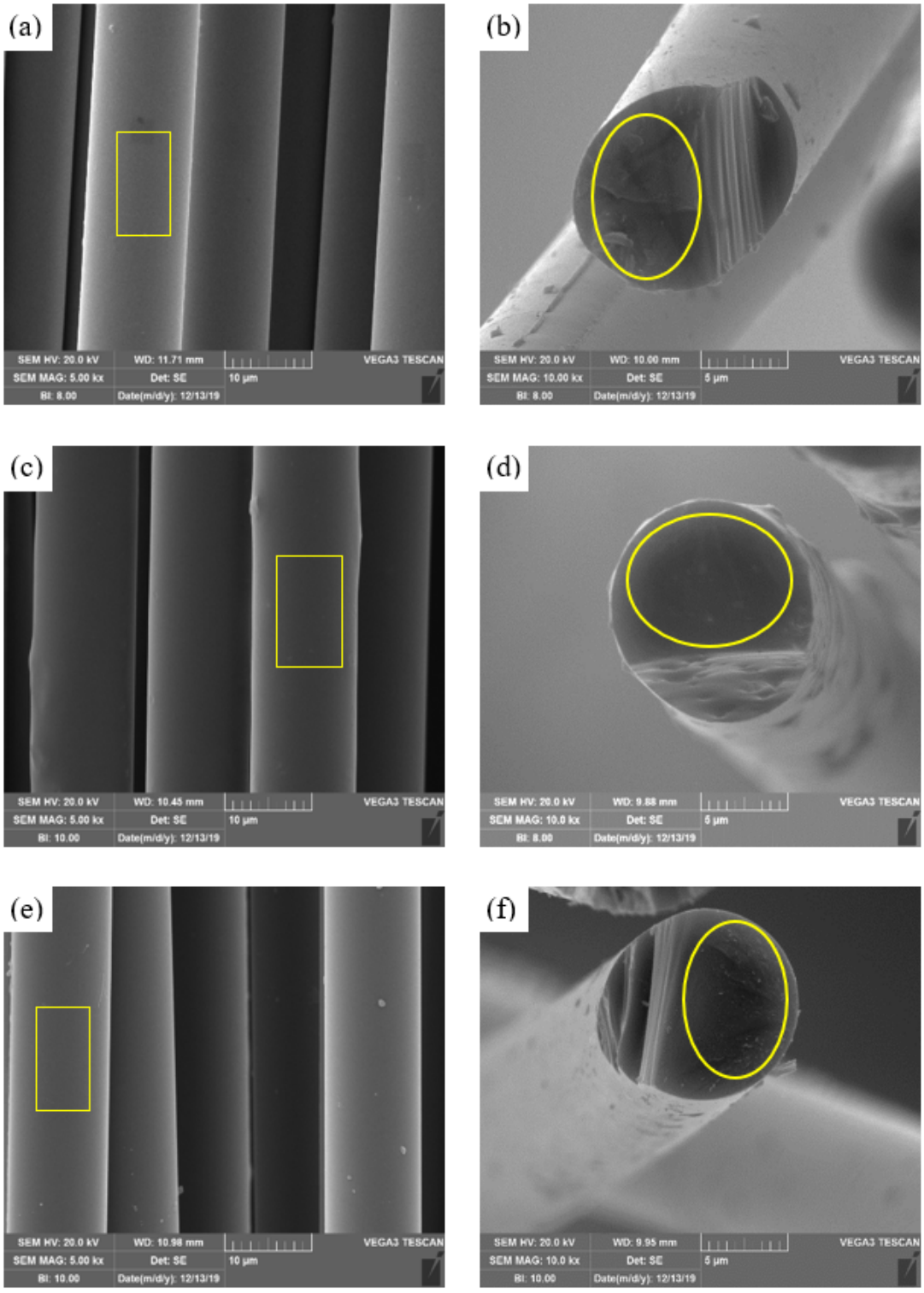

Figure 1

The surface and cross-section morphologies of SLF (a, b), KD-II (c, d) and KD-S (e, f)

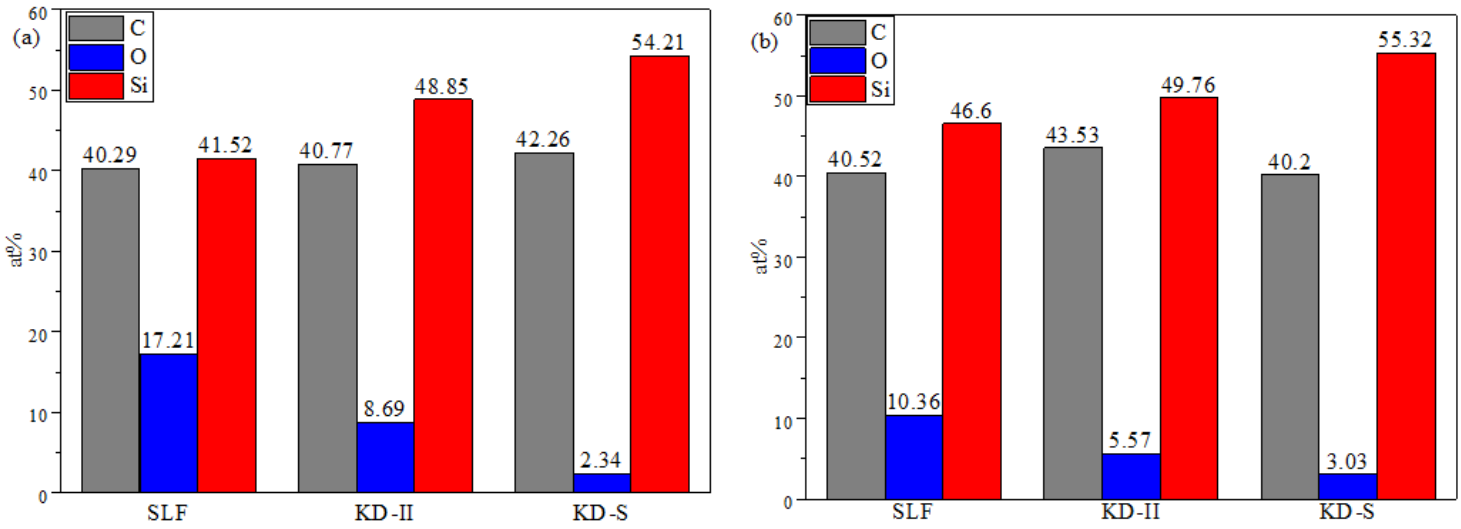

Figure 2

Compositional elements analyzed of surface (a) and cross-section (b) of SLF, KD-II and KD-S SiC fibers by EDS

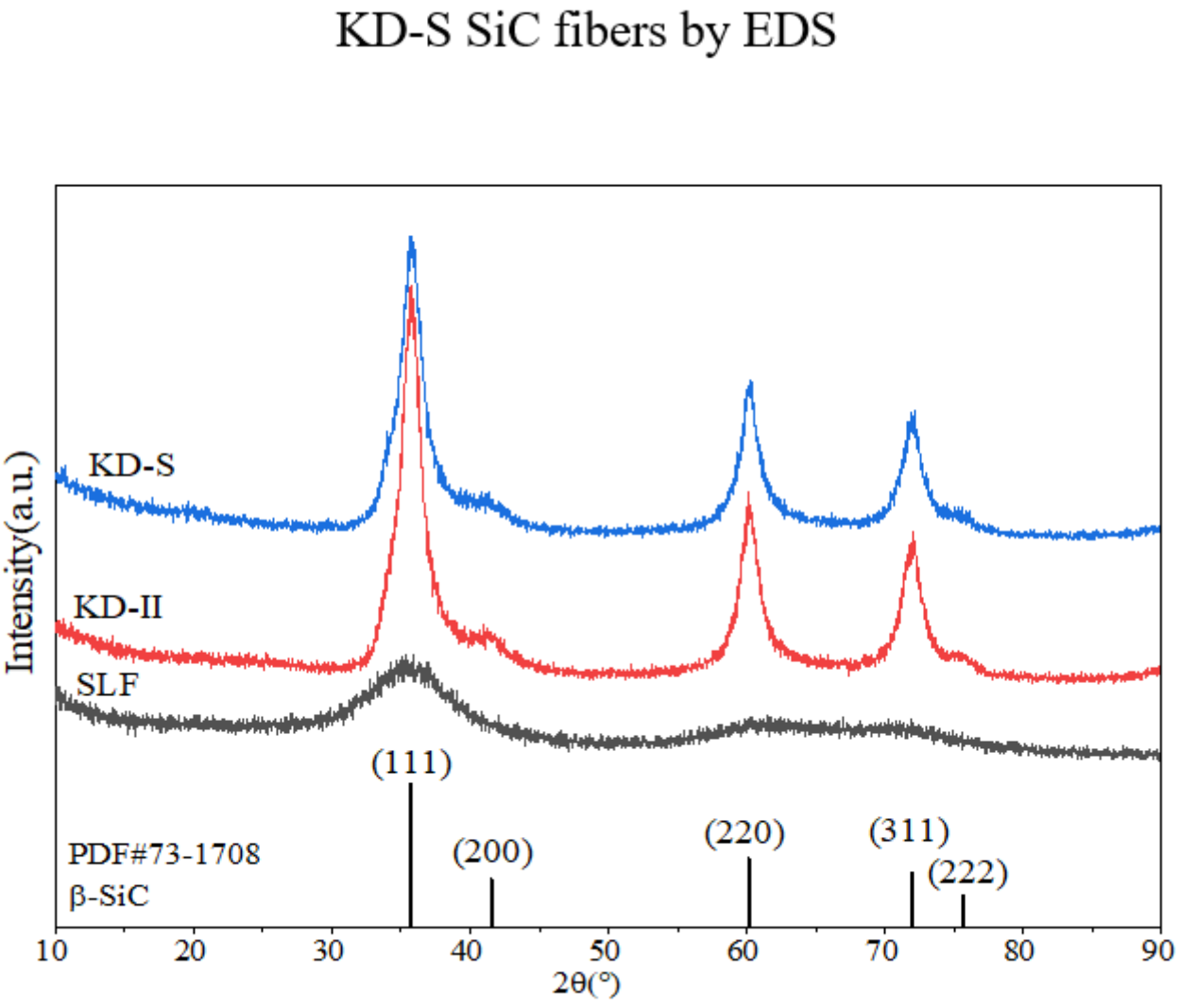

Figure 3

XRD spectra of the SLF, KD-II and KD-S SiC fibers

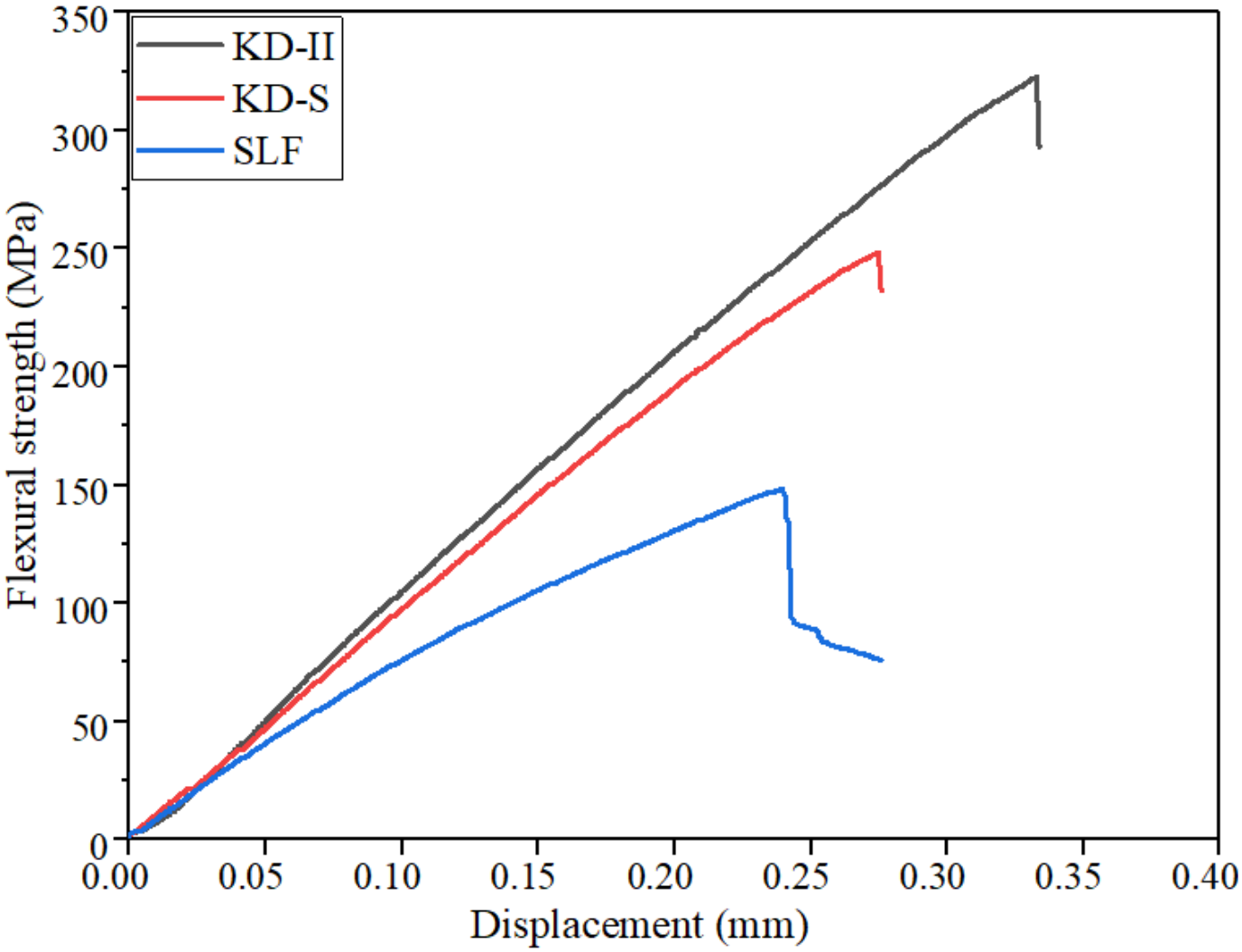

Figure 4

Stress-displacement curves of SiCf/SiC composites with SLF, KD-II and KD-S SiC fibers

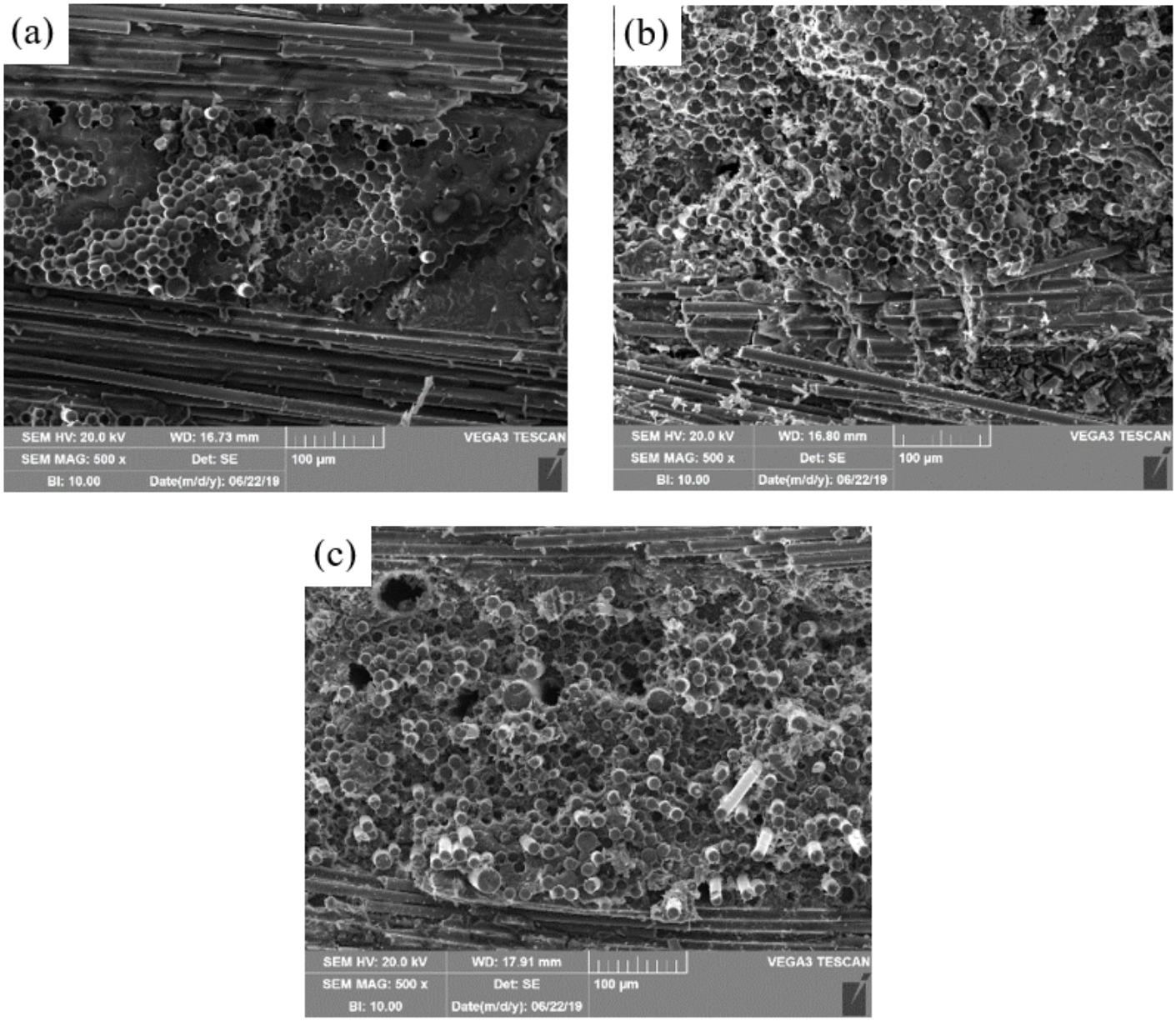

Figure 5

Fracture surface morphologies of SiCf/SiC composites with different SiC fibers (a) SLF, (b) KD-II and (c) KD-S.

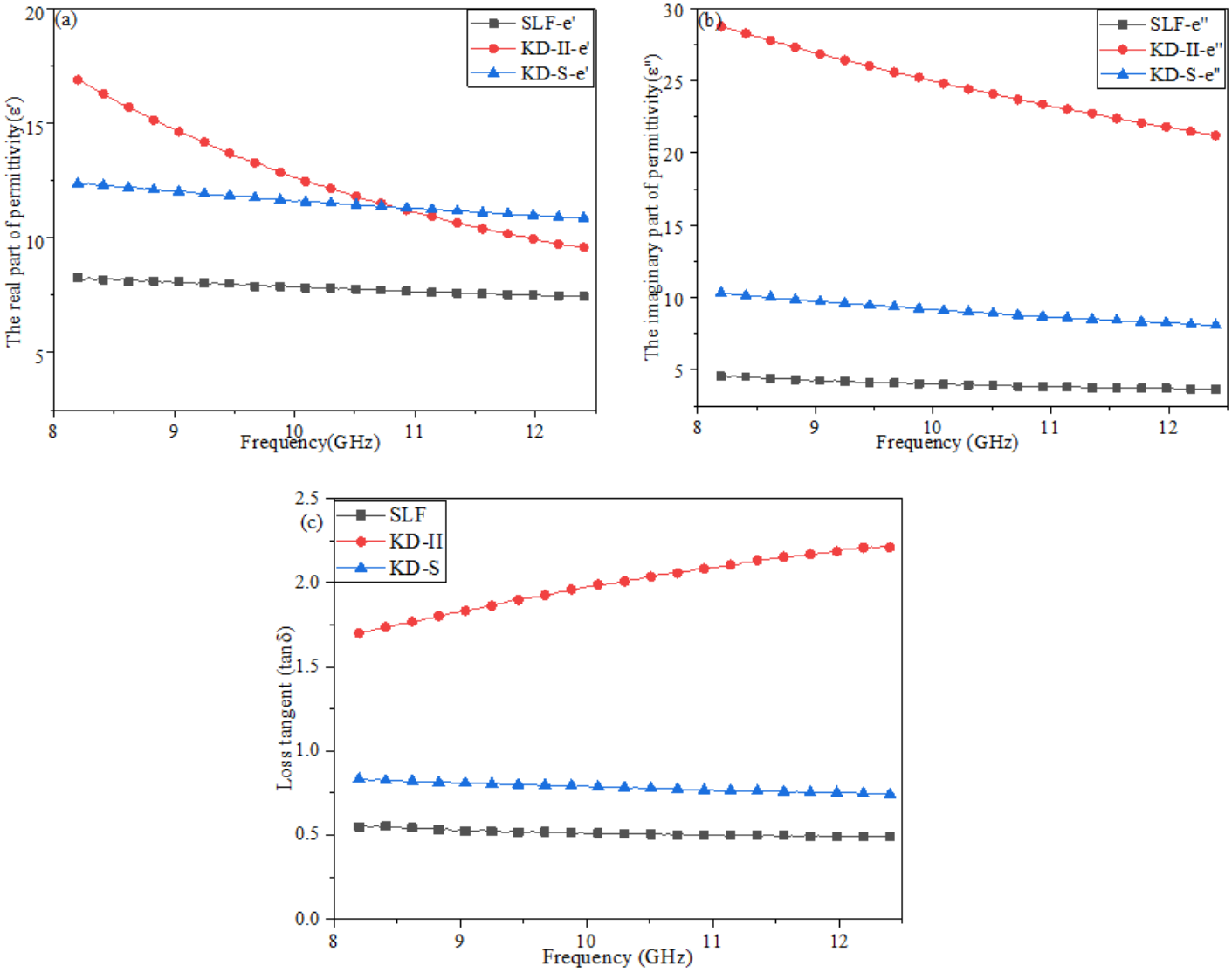

Figure 6

The real (a), imaginary (b) part of complex permittivity and loss tangent (c) for SiCf/SiC composites with SLF, KD-II and KD-S SiC fibers

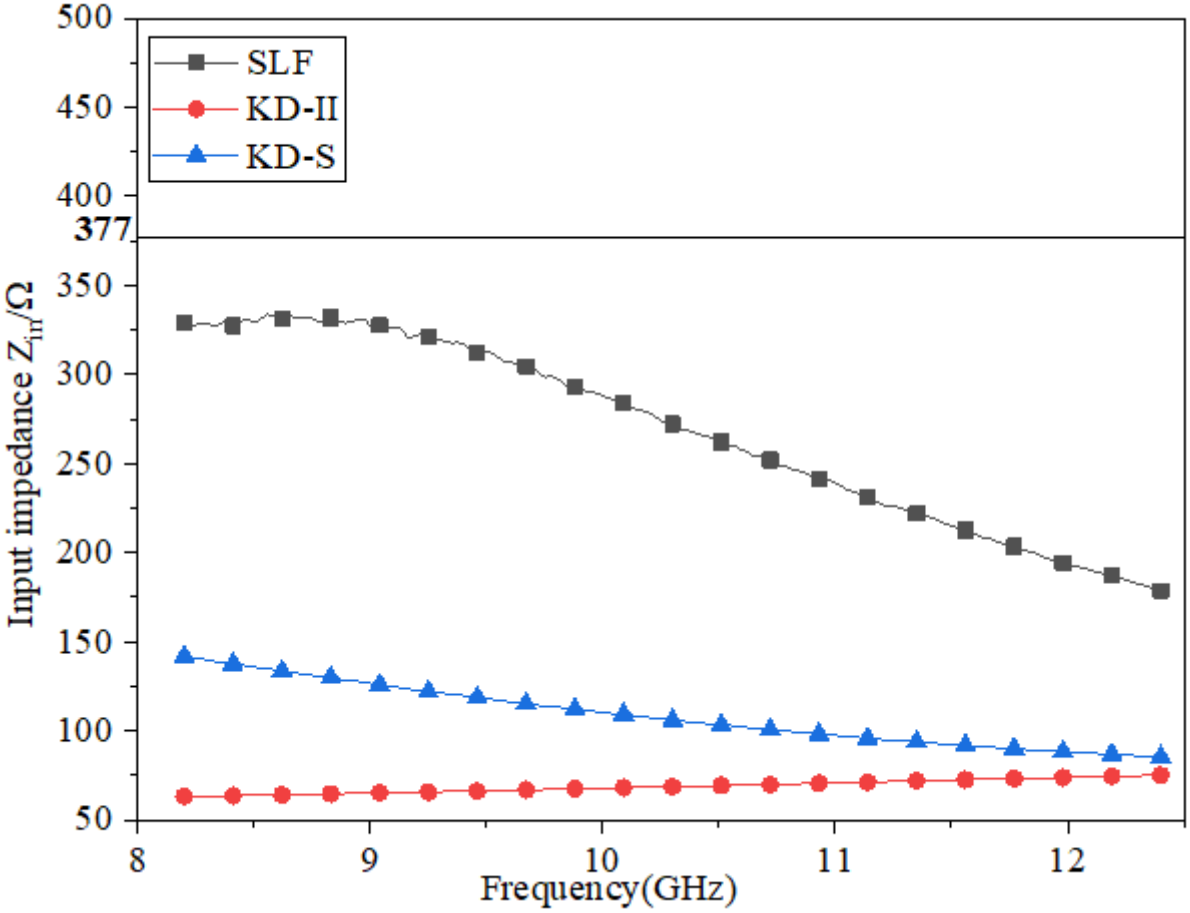

Figure 7

The characteristic input impedance of SLF, KD-II and KD-S SiCf/SiC composites

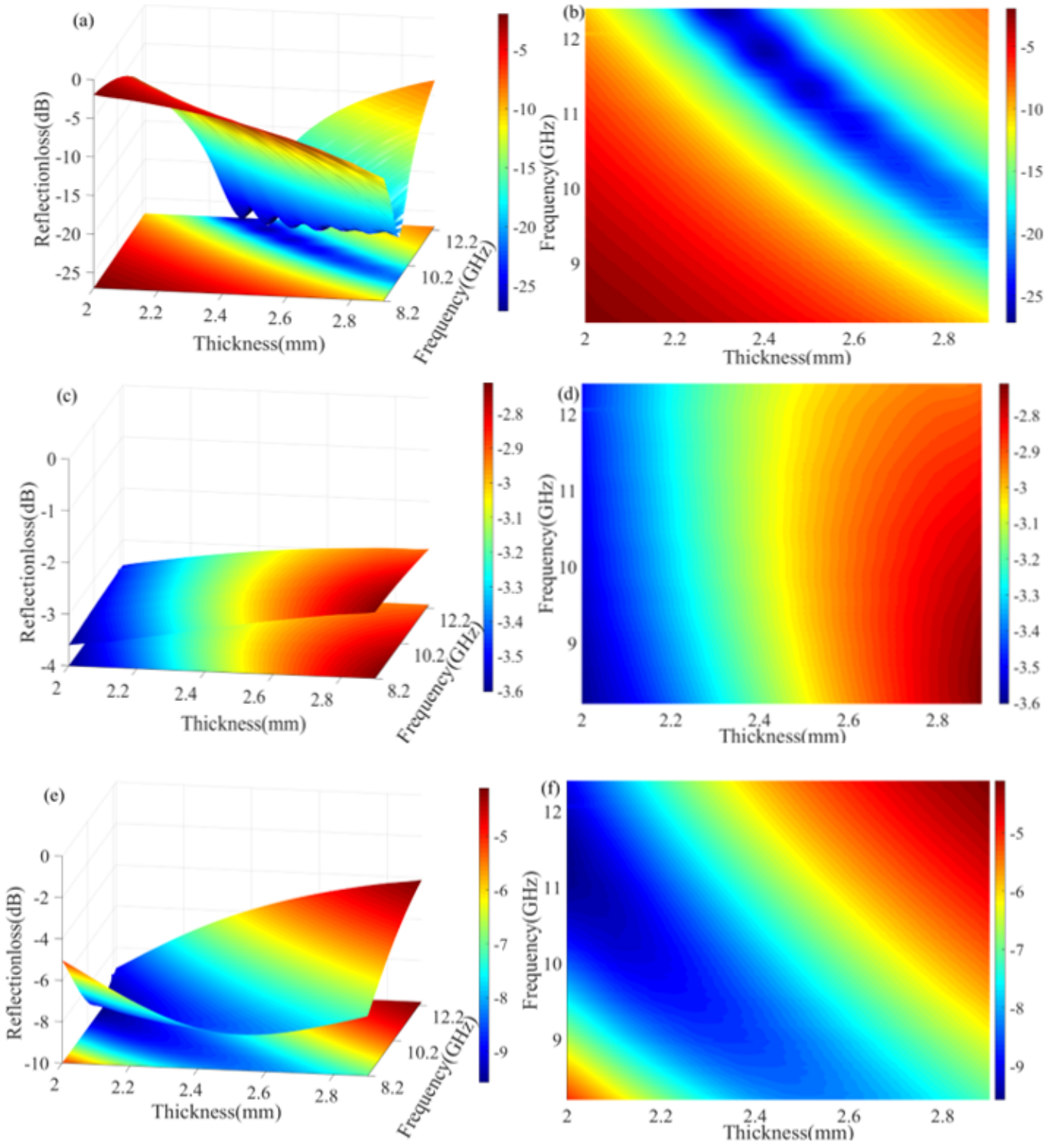

Figure 8

Three-dimensional and detailed maps of RL for SiCf/SiC composites with SLF (a, b), KD-II (c, d) and KD-S (e, f) SiC fibers